Since January 2020 Elsevier has created a COVID-19 resource centre with free information in English and Mandarin on the novel coronavirus COVID-19. The COVID-19 resource centre is hosted on Elsevier Connect, the company's public news and information website.

Original Investigation

Thorax Magnetic Resonance Imaging Findings in Patients with Coronavirus Disease (COVID-19)

Omer Faruk Ates, MD, Onur Taydas, MD, Hamad Dheir, MD

Rationale and Objectives: The aim of this study was to compare the findings found in thorax computed tomography (CT), which is increasingly used in the diagnosis of the important public health problem of coronavirus disease (COVID-19), and the findings of magnetic resonance imaging (MRI) as an important diagnostic alternative.

Materials and Methods: Thirty-two patients diagnosed with COVID-19 who underwent thorax CT for COVID pneumonia and MRI for any reason within 24 hours after CT were included in the study. The number of lobes affected, number of lobes containing ground-glass opacities and consolidation, number of nodules, distribution of lesions (central, peripheral, or diffuse), lobes with centrilobular nodular pattern, and the presence of pleural effusion were recorded separately for both imaging methods.

Results: Seventeen of the patients were female (53%) and 15 were male (47%). The mean age of the patients was 60.5 (range, 20–85) years. A total of 31 patients (96%) had signs of pneumonia on CT. The most common finding in CT was ground-glass opacities in 29 patients (90.6%), followed by consolidation in 14 patients (43.75%). Both consolidation and ground-glass opacities were also observed in MRI in all of these patients. Nodules were detected in 12 patients (37.5%) on CT and 11 patients (34.4%) on MRI. The sensitivity and specificity of MRI in nodule detection were calculated as 91.67% and 100%, respectively.

Conclusion: Although thorax CT is widely used in the imaging of COVID-19 infection, due to its advantages, MRI can also be used as an alternative diagnostic tool.

Key Words: COVID-19; Computed tomography; Magnetic resonance imaging.

INTRODUCTION

In 2019, a new corona virus disease (COVID-19) caused by the severe acute respiratory syndrome coronavirus (SARS-CoV-2) was reported in the Wuhan Province of China (1). The disease spread first in China and then over all the world and was declared as a pandemic by the World Health Organization (WHO) (2). The SARS-CoV-2 virus has been shown to enter the cell through angiotensin converting enzyme 2 (ACE-2) receptors in humans. Therefore, the virus first causes interstitial damage in the lungs followed by parenchymal damage (3). Although the most important clinical symptoms are fever and cough, other indications, such as fatigue, headache and shortness of breath can also be seen. However, diagnostic tests are needed because these symptoms are not disease-specific, and the disease can progress rapidly to severe pneumonia (4). Although the real-time reverse transcription polymerase chain reaction (RT-PCR) test for viral nucleic acids in the diagnosis of COVID-19 is the gold standard, computed tomography (CT) has become increasingly more important in the diagnosis (5). However, considering that it contains ionizing radiation, CT should be used as a problem-solving method rather than for screening purposes in patients who are found negative for RT-PCR but present with clinical symptoms (6). Also, the recent consensus statement from the Fleischner Society lists the risk of radiation exposure to the patient as one of the costs that diminish the value of imaging tests (7).

Due to concerns about the effects of ionizing radiation, magnetic resonance imaging (MRI) is emerging CT as the primary cross-sectional imaging method in evaluating many organs. Today, low dose CT scanning protocols are being developed, however, considering COVID-19 pneumonia and similar pandemics that affect a large number of human populations, dose-dependent and dose-independent effects of CT that may occur due to radiation exposure, poses a serious risk in terms of malignancy that may develop after years (8). Although the low proton content and movement artifacts of

Acad Radiol 2020; 27:1373–1378

From the Sakarya University, School of Medicine, Department of Radiology, Sakarya, Turkey (O.F.A., O.T.); Sakarya University, School of Medicine, Department of Internal Medicine, Sakarya, Turkey (H.D.). Received June 15, 2020; revised July 24, 2020; accepted August 9, 2020. **Address correspondence to:** Onur Taydas e-mail: taydasonur@gmail.com

https://doi.org/10.1016/j.acra.2020.08.009

the lung parenchyma make it difficult to evaluate the lung with MRI, with recent advances in MRI scanner technology such as T2-weighted spin-echo PROPELLER MRI sequence (9), it is now possible to overcome many of these challenges. In addition, the low proton content of the lung is, in fact, an advantage in imaging pneumonia because pulmonary consolidation and ground-glass opacities occurring in pneumonia cause an increase in proton and signal intensity, which becomes more pronounced with the background of the adjacent normal signal (10). In addition, cranial MRI is very useful for the evaluation of anosmia which is frequently seen in these patients (11).

The purpose of this study is to describe the thoracic MRI findings of COVID-19 pneumonia with those of CT and to suggest MRI as an attractive alternative imaging modality is specific cases.

MATERIALS AND METHODS

Patient Selection

For this retrospective study, approval was obtained from the ethical committee of our institution.

Of the 1311 patients diagnosed with COVID-19 pneumonia (RT-PCR at least once + clinically confirmed) in our institution between March 27, 2020 and April 13, 32 who underwent thorax CT for COVID pneumonia and MRI for any reason within 24 hours after CT were included in the study. Since one patient did not complete the MRI examination; thus, his images could not be evaluated, but they were added to the image quality evaluation. A total of 32 patients were included in the study, with 17 being female (53%) and 15 being male (47%). The mean age of the patients was 60.5 (range, 20−85) years. All patients had complaints of dry cough and shortness of breath. The patient population has a wide range from patients with mild disease to those in need of intensive care units. However, none of the patients were intubated.

Both CT and MRI scans were for clinical purposes. T2 propeller images were generally obtained during MRI scans for the following reasons: pulmonary MRA obtained for suspicion of pulmonary thromboembolism in some patients with increased d-dimer without renal failure but with limited renal function and patients with suspected cardiac involvement and therefore imaged with cardiac MRI.

MRI examinations

MRI was performed with a 1.5-T system (Signa Voyager; GE Healthcare, Milwaukee, WI) using a phased array body coil. T2-weighted fast spin Echo PROPELLER axial images were obtained with respiratory triggering (triggered by the expiration phase of the respiratory cycle) at an echo train length of 13, matrix of 224 × 256, FOV of 38 cm, band width of 125 Hz, TR of 1000−1500 ms, effective echo time of ~90 ms, and four excitations. Slice thickness was 5 mm, and interslice gap was 1 mm. The imaging time was approximately 3 minutes, but it was extended to 5 minutes in patients with breathing problems.

CT Examinations

CT images were obtained with a 64-row multidetector CT scanner (5 mm slice thickness, matrix of 512 × 512, 120 kV automatically modulated mA; Aquilion64, Toshiba Medical Systems, Japan) for 21 patients and with a 16-row multidetector CT scanner (5 mm slice thickness, matrix of 512 × 512, 120 kV automatically modulated mA, Alexion, Toshiba Medical Systems, Japan) for 11 patients. All scans were performed during inspiration and with the patients placed in the supine position.

Image Analysis

The MRI and CT images of all patients were evaluated for opacity and unilateral or bilateral involvement. The number of lobes affected ($n = 1-5$), number of lobes containing ground-glass and consolidation, number of nodules, distribution of lesions (central, peripheral, or diffuse), lobes with centrilobular nodular pattern, and the presence of pleural effusion were also recorded separately for both imaging methods. On CT and MRI, a density/intensity increase in which vascular boundaries could be distinguished was accepted as ground-glass, and a density/intensity increase in vascular structures that could not be differentiated was considered as consolidation. The affected lung volume ratio was evaluated observationally. By definition, a lung nodule is a rounded or irregular opacity, which may be well or poorly defined, measuring ≤3 cm in diameter.

The CT and MRI images were assessed for quality: 5, excellent no artifacts; 4, good (few artifacts); 3, moderate (of diagnostic value but impaired by artifacts); 2, poor (of no diagnostic value); and 1, not tolerated (examination could not be completed). The causes of impaired quality were attributed to ghosting, motion or patient movement artifacts, or a combination thereof. The evaluation of the images was independently undertaken by two radiologists (both are board-certified and have 8 years of experience) with the prediagnosis of COVID-19-related pneumonia. Two weeks were waited for evaluation of MRI images after evaluation of CT images to prevent memory bias. If their initial opinions differed, a consensus was reached.

Statistical Analysis

MedCalc (ver. 12, Ostend, Belgium) was used for statistical analysis. The descriptive statistics were given as median (minimum − maximum) and mean ± standard deviation. Categorical variables were stated as frequencies and percentages. The chi-square test was used for the comparison of categorical variables. The independent samples *t* test was used for the comparison of continuous variables with normal distribution and the Mann-Whitney *U* and Kruskal Wallis tests for the data that did not conform to normal

distribution in the Kolmogorov-Smirnov test. Coherence between two observers with respect to pulmonary findings was assessed by Cohen's Kappa coefficient. A value of $p < 0.05$ was accepted as statistically significant.

RESULTS

A total of 31 patients (96%) had signs of pneumonia on CT. Pneumonia findings were observed in the MRI of these patients. The most common involvement pattern was bilateral and peripheral (Table 1; Fig 1). Almost perfect agreement was found between the two observers in terms of pulmonary findings ($\kappa = 0.934$).

The most common finding in CT was ground-glass opacities in 29 patients (90.6%). Ground-glass opacities were also observed in the MRI of all of these patients. Lesions were observed in one or two lobes most frequently in both CT and MRI (37.5%) (Figs 2 and 3). While a total of 90 lesions were detected on CT, 85 were detected on MRI, but there was no statistically significant difference ($p = 0.710$) (Table 2). The second most frequently observed finding in CT was consolidation in 14 patients (43.75%), which was also observed in the same patients on MRI. Lesions were detected in one or two lobes most frequently in both CT and MRI (25%) (Table 3). Nodules were detected in 12 patients (37.5%) by CT and 11 patients (34.4%) by MRI. Taking CT as reference, the sensitivity of MRI in nodule detection was calculated as 91.7%, specificity 100%, positive predictive value 100%, and negative predictive value 95.2%. While 53 nodules were observed in CT, 52 were observed in MRI, and no significant difference was found between the two modalities ($p = 0.967$) (Figs 4 and 5). In addition, on both CT and MRI, three patients (9.4%) had a centrilobular nodular pattern (Fig 6) and eight (25%) had pleural effusion.

The median image quality score was 5 for the CT images and 4 for the MRI images (Table 4). However, there was no significant difference between the two imaging methods ($p = 0.147$).

TABLE 1. Comparison of Findings Observed in CT and MRI

	CT		MRI	
	N	%	*n*	%
Lung involvement	31	96.9	31	96.9
Unilateral	8	25	8	25
Bilateral	23	71.9	23	71.9
Affected lobes				
1	6	18.8	7	21.9
2	5	15.6	5	15.6
3	4	12.5	3	9.4
4	4	12.5	5	15.6
5	12	37.5	11	34.4
Location of lesion				
Peripheral	21	65.6	21	65.6
Central	1	3.1	1	3.1
Diffuse	9	28.1	9	28.1

DISCUSSION

The most important result of our study is the nearly complete overlap of CT and MRI findings. Minor differences between CT and MRI may have been influenced by the fact that CT scanning is obtained during the inspiratory phase of respiration and thoracic MRI with respiratory navigator during expiratory phase. In this context, MRI was shown to be a useful modality in terms of showing both parenchymal and extraparenchymal (pleural effusion and lymphadenopathy) findings. In a recent study involving 23 patients by Yang et al., ultrashort echo time MRI was evaluated and compared to CT. In this study, similar to our study, a perfect match was found between MRI findings and CT findings. However, the most important difference of this study from our study is that no patient with a nodule was included in the study (12). There are also two case reports in the literature regarding the MRI findings of COVID-19. The first belonged to a 47-year-old male patient and both parenchymal consolidation and pleural effusion was demonstrated using MRI (13). The other case report described a 33-year-old male patient, who was shown to have parenchymal ground-glass densities and consolidations successfully revealed by MRI (14).

Various findings can be seen in the lung parenchyma in COVID-19 infection (15). The most common of these is the ground-glass appearance, defined as an increase in fog-shaped density in which the walls of the vessels and bronchi are not wiped (16,17). It develops due to mild interstitial thickening or air loss within the airways (18). In a meta-analysis performed by Salehi et al. involving 919 patients, ground-glass density was determined in 88% of patients and reported as the most common imaging finding (19). In a study conducted in Italy, all patients were found to have ground-glass density (20). Similarly, in our study, all patients had ground-glass opacities. It is also known that ground-glass density is the earliest radiological finding of the disease (21). This appearance is considered to be due to edema and hyaline membranes in the lung (22). Ground-glass opacities can be seen alone or together with different findings, such as interlobular septal thickening and consolidation (23). Consolidation is defined as the air in the alveoli being completely replaced with pathological fluid, cells or tissues, resulting in an increase in density, and it is usually multifocal, segmental, patchy and subpleural or peribroncovascular in patients with COVID-19 infection (24). In our study, there was consolidation in 43.75% of patients. Pathophysiologically, these cases are thought to be associated with fibromixoid exudate in the alveoli (25). In addition, the presence of consolidation has been associated with the prognosis of the ailment and may be an indicator of a progressive disease (23). Crazy paving, which is defined as thickened interlobular and intralobular septa and the background with ground-glass density, is important because it is a sign of a progressive disease, although it is not as common as

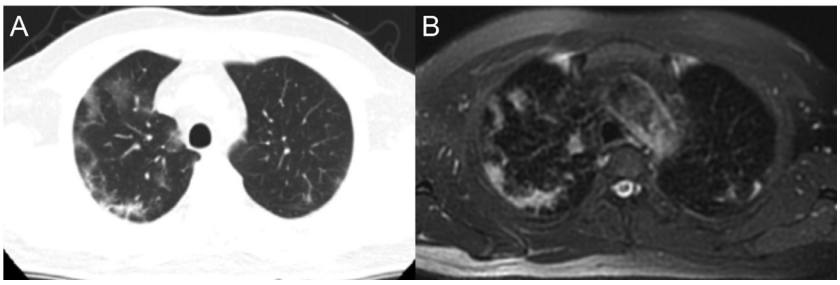

Fig. 1. Images of a 50-year-old male, showing ground-glass areas with bilateral peripheral distribution similarly visualized on both computed tomography (a) and magnetic resonance imaging (b).

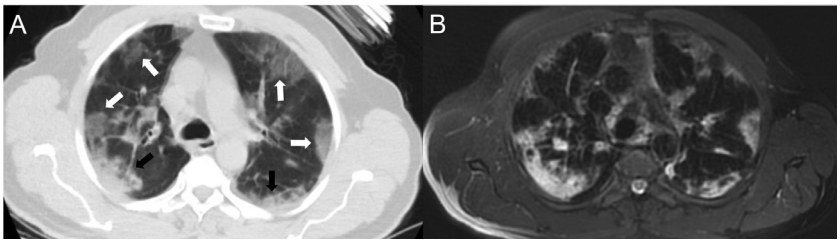

Fig. 2. Images of an 81-year-old woman with peripheral-weighted diffuse involvement. In areas where there are ground-glass appearances (white arrows) on both CT (a) and MRI (b), vascular structures can be selected, while in the consolidated areas, vascular structures cannot be distinguished (black arrows).

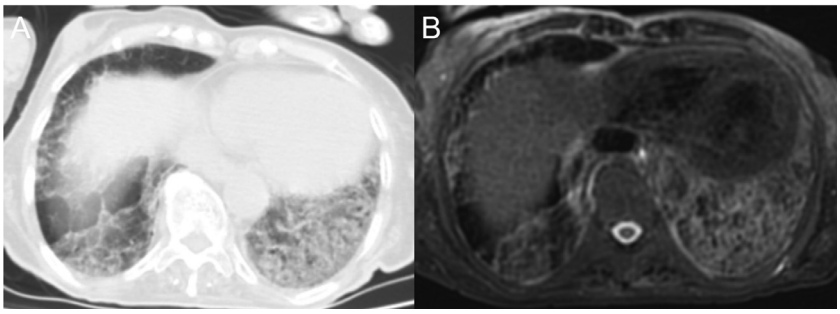

Fig. 3. Crazy-paving pattern in an 81-year-old male patient. Interlobular and intralobular septal thickening and ground-glass appearance are displayed very successfully by MRI (b), as well as CT (a).

TABLE 2. Lobar Distribution in Patients with Ground-Glass Opacity

Number of Affected Lobes	CT		MRI		*p*
	n	%	*n*	%	
0	3	9.4	3	9.4	
1	6	18.8	7	21.9	
2	6	18.8	5	15.6	
3	4	12.5	4	12.5	
4	5	15.6	9	28.1	
5	8	25	4	12.5	
Total	90		85		0.710

TABLE 3. Lobar Distribution in Patients with Consolidation

Number of Affected Lobes	CT		MRI	
	n	%	*n*	%
0	18	56.3	18	56.3
1	3	9.4	3	9.4
2	5	15.6	5	15.6
3	3	9.4	3	9.4
4	3	9.4	3	9.4
5	0	0	0	0
Total	34		34	

consolidation and ground-glass in COVID-19 infection (26). Apart from these major findings, a reticular pattern, air bronchogram, and nodules can also be seen (18). Lymphadenopathy and pleural effusion are rarely observed in COVID-19 infection and tends to suggest a bacterial infection in RT-PCR positive patients (18).

The use of thorax MRI has been increasing in recent years. Since there is no radiation risk, MRI allows multiple examinations to be performed on the same patient, and it can provide additional information to CT during patient follow-up. In a study by Leutner et al., in which 16 immunocompromised patients with pneumonia were included, all ground-glass opacities and consolidations could be diagnosed with MRI. Moreover, the presence of early-stage necrotic pneumonia, which could not be shown by contrast-enhanced CT in 25% of patients, was demonstrated by MRI (27). In subsequent studies with a similar patient group, MRI was found to be very useful diagnostic tool, especially in its use during follow-up (28,29); furthermore, MRI was reported to be promising in detecting nodules in these patients (30). In our study, the sensitivity of MRI in nodule detection was 91.67%, and its specificity was 100%. In a recent study by Syrjala et al. including 77 patients with immunocompetent pneumonia, the effectiveness of MRI in diagnosis was investigated, and it was reported that MRI was superior to direct radiography in diagnosis and showed almost identical accuracy with CT (31).

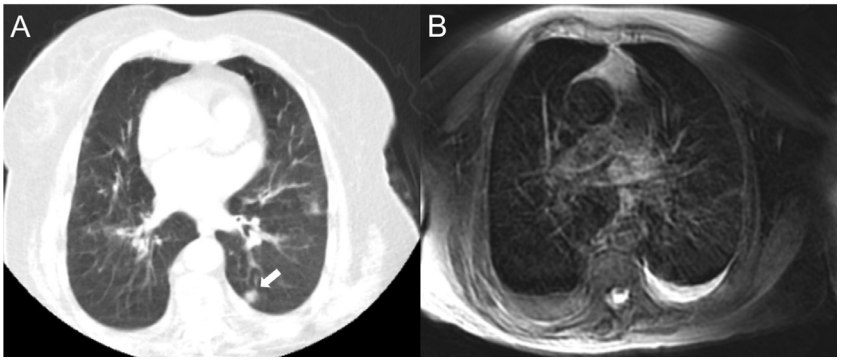

Fig. 4. An 82-year-old female patient with heart failure and chronic obstructive pulmonary disease, presenting with a nodule in the superior segment of the left lung lower lobe displayed clearly on CT (a, arrow), but with poorer quality on MRI (b) due to intense artifacts.

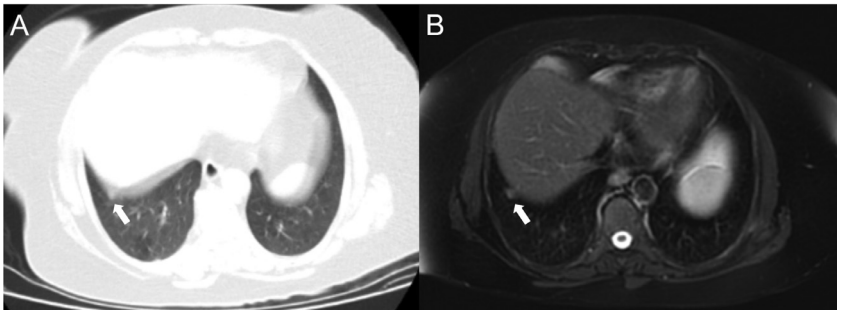

Fig. 5. A 59-year-old female patient presenting with a nodule (arrow) that is considerably affected by a motion artifact due to its adjacency to the diaphragm in CT examination (a) but can be easily seen on the T2 FSE PROPELLER MRI image due to respiratory gating (b).

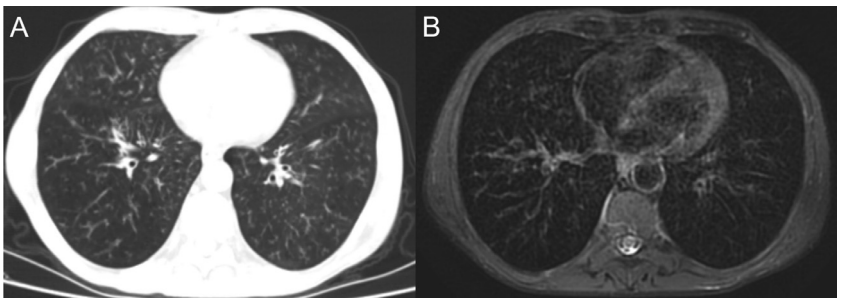

Fig. 6. A 61-year-old male patient with a centrilobular nodular pattern, which is one of the rare findings in COVID-19-related pneumonia. Although the nodules are easier to distinguish on CT, this pattern is also shown very successfully on the MRI image.

TABLE 4. Comparison of CT and MRI Image Quality

Image Quality Score	CT		MRI	
	n	%	*n*	%
1 (Not completed)	0	0	0	0
2 (Poor)	0	0	1	3.1
3 (Moderate)	6	18.8	6	18.8
4 (Good)	8	25	14	43.8
5 (Excellent)	18	56.3	11	34.4

One of the disadvantages of MRI in pneumonia patients is imaging time and artifacts. In addition to longer scan times, MR is less readily available and more expensive than CT. In our routine practice, we use the PROPELLER technique, which has been shown to obtain better quality and less artifact images, while taking the thorax image (9). The T2 FSE PROPELLER sequence used in our study lasted an average of 3 minutes. Shortness of breath, which can be seen in patients with COVID-19-related pneumonia, can cause an increase in both CT and MRI in motion-related artifacts. At the same time, since this sequence is obtained with a respiratory navigator, the scanning time is prolonged in patients with irregular breathing. Although it is more sensitive to motion artifacts due to the long scanning time, respiratory navigation may be an advantage, especially in the imaging of some lesions adjacent to the diaphragm. In breath-hold CT, since inferior slices are taken toward the end of the patient's breath, more intense motion artifacts occur, especially in the inferior slices in patients with shortness of breath. In the technique we use, even the lesions adjacent to the diaphragm can be easily viewed in patients who regularly breathe quickly, as it is not necessary for them to hold their breath. Although CT was better in terms of overall image quality in our study, there was no significant difference between the CT and MRI examinations. In addition, no artifact formation at the level of no diagnosis was observed in the MRI of any patient. In addition, no artifact formation at level 2 (poor image quality, of no diagnostic value) was observed in any patient on MRI.

There were some limitations of our study. The first was the small number of patients included in the study, and second was the retrospective nature of the research. More comprehensive and prospective studies can be planned for this subject. Finally, since the MRI examinations were performed

without contrast, the effect of the contrast agent could not be evaluated.

In conclusion, although thorax CT is widely used in the imaging of COVID-19 infection, we consider that MRI can be used as an alternative due to its various advantages. Especially, MRI is important to assess lung pathology over time as more is learned about COVID and the long-term impact on lung health. T2-weighted spin-echo PROPELLER sequence, variations of which are readily-available sequence on most MRI scanners, is a good option for clinical translation to other platforms, sites.

ETHICS

This retrospective study has been approved by the local ethics committee and conducted in accordance with the Declaration of Helsinki.

FINANCIAL DISCLOSURE

The authors declared that this study has received no financial support.

CONFLICT OF INTEREST

The authors declare no conflict of interests.

REFERENCES

1. Zhu N, Zhang D, Wang W, et al. A novel coronavirus from patients with pneumonia in China, 2019. N Engl J Med 2020; 382:727–733.
2. COVID C, Team R. Severe outcomes among patients with coronavirus disease 2019 (COVID-19)—United States, February 12–March 16, 2020. MMWR Morb Mortal Wkly Rep 2020; 69:343–346.
3. Xu X, Chen P, Wang J, et al. Evolution of the novel coronavirus from the ongoing Wuhan outbreak and modeling of its spike protein for risk of human transmission. Sci China Life Sci 2020; 63:457–460.
4. Akcay MS. Radiological approaches to Covid-19 pneumonia. Turk J Med Sci 2020.
5. Huang C, Wang Y, Li X, et al. Clinical features of patients infected with 2019 novel coronavirus in Wuhan, China. Lancet 2020; 395:497–506.
6. Erturk SM. CT of coronavirus disease (COVID-19) pneumonia: a reference standard is needed. AJR Am J Roentgenol 2020. W1.
7. Rubin GD, Ryerson CJ, Haramati LB, et al. The role of chest imaging in patient management during the COVID-19 pandemic: a multinational consensus statement from the Fleischner society. Radiology 2020; 296:172–180.
8. Mathews JD, Forsythe AV, Brady Z, et al. Cancer risk in 680,000 people exposed to computed tomography scans in childhood or adolescence: data linkage study of 11 million Australians. Bmj 2013; 346:f2360.
9. Meier-Schroers M, Kukuk G, Homsi R, et al. MRI of the lung using the PROPELLER technique: Artifact reduction, better image quality and improved nodule detection. Eur J Radiol 2016; 85:707–713.
10. Liszewski MC, Gorkem S, Sodhi KS, et al. Lung magnetic resonance imaging for pneumonia in children. Pediatr Radiol 2017; 47:1420–1430.
11. Galougahi MK, Ghorbani J, Bakhshayeshkaram M. Olfactory bulb magnetic resonance imaging in SARS-CoV-2-induced anosmia: the first report. Acad Radiol 2020; 27:892–893.
12. Yang S, Zhang Y, Shen J, et al. Clinical potential of UTE-MRI for assessing COVID-19: patient- and lesion-based comparative analysis. J Magn Reson Imaging 2020.
13. Langenbach MC, Hokamp NG, Persigehl T, et al. MRI appearance of COVID-19 infection. Diagn Interv Radiol 2020.
14. Fonseca EKUN, Chate RC, Neto RS, et al. Findings of COVID-19 on magnetic resonance imaging. Radiology 2020; 2:e200193.
15. Li M, Lei P, Zeng B, et al. Coronavirus disease (COVID-19): spectrum of CT findings and temporal progression of the disease. Acad Radiol 2020; 27:603–608.
16. Wan S, Li M, Ye Z, et al. CT manifestations and clinical characteristics of 1115 patients with coronavirus disease 2019 (COVID-19): a systematic review and meta-analysis. Acad Radiol 2020; 27:910–921.
17. Guan CS, Lv ZB, Yan S, et al. Imaging features of coronavirus disease 2019 (COVID-19): evaluation on thin-section CT. Acad Radiol 2020; 27:609–613.
18. Ye Z, Zhang Y, Wang Y, et al. Chest CT manifestations of new coronavirus disease 2019 (COVID-19): a pictorial review. Eur Radiol 2020.
19. Salehi S, Abedi A, Balakrishnan S, et al. Coronavirus disease 2019 (COVID-19): a systematic review of imaging findings in 919 patients. AJR Am J Roentgenol 2020: 1–7.
20. Caruso D, Zerunian M, Polici M, et al. Chest CT features of COVID-19 in Rome, Italy. Radiology 2020:201237.
21. Chung M, Bernheim A, Mei X, et al. CT imaging features of 2019 novel coronavirus (2019-nCoV). Radiology 2020; 295:202–207.
22. Xu Z, Shi L, Wang Y, et al. Pathological findings of COVID-19 associated with acute respiratory distress syndrome. Lancet Respir Med 2020; 8:420–422.
23. Song F, Shi N, Shan F, et al. Emerging 2019 novel coronavirus (2019-nCoV) pneumonia. Radiology 2020; 295:210–217.
24. Wu J, Wu X, Zeng W, et al. Chest CT findings in patients with coronavirus disease 2019 and its relationship with clinical features. Invest Radiol 2020; 55:257–261.
25. Shi H, Han X, Jiang N, et al. Radiological findings from 81 patients with COVID-19 pneumonia in Wuhan, China: a descriptive study. Lancet Infect Dis 2020; 20:425–434.
26. Wong KT, Antonio GE, Hui DS, et al. Thin-section CT of severe acute respiratory syndrome: evaluation of 73 patients exposed to or with the disease. Radiology 2003; 228:395–400.
27. Leutner CC, Gieseke J, Lutterbey G, et al. MR imaging of pneumonia in immunocompromised patients: comparison with helical CT. AJR Am J Roentgenol 2000; 175:391–397.
28. Ekinci A, Yucel Ucarkus T, Okur A, et al. MRI of pneumonia in immunocompromised patients: comparison with CT. Diagn Interv Radiol 2017; 23:22–28.
29. Singh R, Garg M, Sodhi KS, et al. Diagnostic accuracy of magnetic resonance imaging in the evaluation of pulmonary infections in immunocompromised patients. Polish J Radiol 2020; 85:e53–e61.
30. Ozcan HN, Gormez A, Ozsurekci Y, et al. Magnetic resonance imaging of pulmonary infection in immunocompromised children: comparison with multidetector computed tomography. Pediatr Radiol 2017; 47:146–153.
31. Syrjala H, Broas M, Ohtonen P, Jartti A, Paakko E. Chest magnetic resonance imaging for pneumonia diagnosis in outpatients with lower respiratory tract infection. Eur Respir J 2017: 49.